Original Article

Electrochemical behavior of dissolved hydrogen at Pt electrode surface in a high temperature LiOH−H₃BO₃ solution: Effect of chloride ion on the transient current of the dissolved hydrogen

Myung-Hee Yun, Jei-Won Yeon[*]

Nuclear Chemistry Technology Division, Korea Atomic Energy Research Institute, 111, Daedeok-daero 989beon-gil, Yuseong-gu, Daejeon, 34057, Republic of Korea

A B S T R A C T

The electrochemical behavior of dissolved hydrogen (H_2) was investigated at a Pt electrode in a high temperature LiOH−H₃BO₃ solution. The diffusion current of the H_2 oxidation was proportional to the concentration of the dissolved H_2 as well as the reciprocal of the temperature. In the polarization curve, a potential region in which the oxidation current decreases despite an increase in the applied potential between the H_2 oxidation and the water oxidation regions was observed. This potential region was interpreted as being caused by the formation of a Pt oxide layer. Using the properties of the Cl^- ion that reduces the growth rate of the Pt oxide layer, it was confirmed that there is a correlation between the Cl^- ion concentration and the transient current of the H_2 oxidation.

© 2023 Korean Nuclear Society, Published by Elsevier Korea LLC. This is an open access article under the CC BY-NC-ND license (http://creativecommons.org/licenses/by-nc-nd/4.0/).

1. Introduction

Hydrogen gas (H_2) is one of the most important chemical additives in the nuclear reactor coolant system [1,2]. H_2 dissolved in the coolant mitigates the corrosion of structural materials by suppressing the radiolysis of water molecules and keeping the coolant in the reducing condition. The dissolved H_2 can also affect the cracking of the Zircaloy cladding [3−5], the stress corrosion of steam generator tubes [6,7] and the deposition of corrosion products [8,9]. As described above, it is clear that dissolved H_2 has various effects on the safe operation of the reactor coolant system and is an essential additive.

On the other hand, Pt is a stable noble metal and has been used as a reaction catalyst and an electrochemical sensor material for a long time because it has unique surface reaction characteristics. Although many studies [10−13] have been conducted on various electrochemical reactions involving dissolved H_2 on the Pt surface at room temperature, they are still insufficient in terms of providing experimental data and electrochemical behavior. This is due to

difficulties in maintaining conditions and applying electrochemical techniques at high temperatures. Since Pt is very stable in high temperature water, the high temperature electrochemical behavior of the dissolved H_2 at Pt electrodes will be useful for developing Pt-based sensors along with an understanding of high temperature water chemistry.

We have previously reported [14] on the high temperature oxidation behavior of H_2 at Pt electrodes. In the 473 K experiment, a peculiar potential region with a minimum current value was observed between the dissolved H_2 oxidation and the water oxidation potential regions at the Pt electrode. This phenomenon was explained by the formation of a Pt oxide layer [14]. We also mentioned the possibility of Cl^- concentration monitoring using the transient behavior of H_2 oxidation [15]. However, the previous studies only briefly reported the observation of this peculiar phenomenon and the possibility of Cl^- concentration monitoring, so there was not detailed analysis on the high temperature behavior of H_2 oxidation, the formation of the Pt oxide layer, and the effects of the Cl^- ions. Actually, not only Cl^- ions but also halide ions such as bromide and iodide will make it difficult to form a Pt oxide layer, but we first investigated Cl^- ions which may exist in a nuclear reactor coolant system.

In this study, the oxidation behavior of H_2 was analyzed in more

detail in the temperature range of 298–553 K and the H_2 concentration of $0-4 \times 10^{-4}$ M. Through this, a relationship between the diffusion current of H_2 and the temperature was derived, and additional analysis was performed on the potential region to form a Pt oxide layer that inhibits H_2 oxidation. In addition, the Cl^- ion concentration and dissolved H_2 oxidation current were compared in steady-state and transient conditions, and the correlation between the Cl^- concentration and transient current was newly interpreted by reflecting the formation of the Pt oxide layer. This study will help to understand the effect of impurities such as Cl^- ions on the oxidation behavior of dissolved H_2 and the formation rate of Pt oxide layer at high temperatures.

2. Materials and methods

A loop system was used to investigate the high temperature behavior of dissolved H_2 on a Pt surface. The loop system basically consisted of a high temperature electrochemical cell, a potentiostat system, and a rod-type electric heater, as shown in Fig. 1. The linear flow rate and pressure of the loop solution were adjusted to 0.5 cm min^{-1} and 15 MPa, by using a metering pump (Teikoku) and a back pressure regulator (Tescom). The loop solution was prepared by mixing the reagent grade LiOH and H_3BO_3, and the solution temperature was controlled in the range of 298–553 K with a rod-type electric heater. The solution temperature was only controlled between the electric heater and the water cooling jacket, and the other parts were controlled at room temperature.

Before the electrochemical experiments, we confirmed the dissolved H_2 concentration in the loop could be controlled in the range of $0.32-4.0 \times 10^{-4}$ M by using H_2/Ar mixed gas with H_2

fractions of 0%, 4%, 10%, 20%, and 50%, respectively. The H_2 concentration values (in loop) measured by a hydrogen analyzer (Orbisphere) were compared to the H_2 concentration values calculated from the H_2 partial pressure (in reservoir). By the comparison, it was confirmed that the dissolved H_2 concentration in the loop was accurately proportional to the H_2 partial pressure in the reservoir. After confirming this proportional relationship, the dissolved H_2 concentration in the loop was calculated by the H_2 fractions of the mixed gas.

In the electrochemical system, a Pt rod and a Pt wire with a diameter of 1 mm were used as the working and counter electrodes, respectively. The exposed areas of the working and counter electrodes were respectively 0.1 cm^2 and ~2 cm^2. And a 0.1 M KCl Ag/AgCl electrode (Cormet) was used as an external reference electrode. Potentiodynamic polarization and potential transient techniques were employed to investigate the electrochemical behavior of the dissolved H_2 and to detect chloride ions in the hydrogenated solution. Electrochemical measurements were performed using a potentiostat system (Bio-Logic SAS) and controlled by application software (EC-Lab). All the electrochemical potentials used in this study represent the actual applied potentials based on the external reference electrode without correcting the thermal liquid junction potential.

3. Results and discussion

3.1. Effect of temperature on the electrochemical behavior of dissolved H_2

Fig. 2a shows the potentiodynamic polarization curves of the Pt
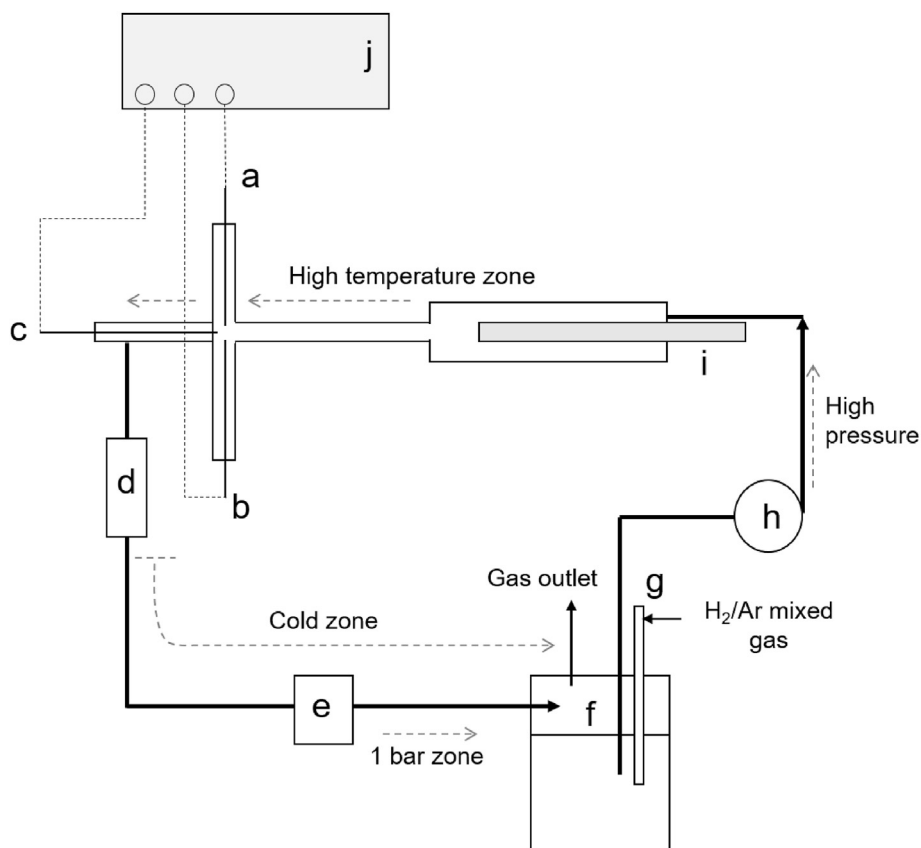
Fig. 1. Scheme of high temperature electrochemical measurement loop system: a) Pt working electrode; b) Ag/AgCl external reference electrode; c) Pt counter electrode; d) water cooling jacket; e) back pressure regulator (BPR); f) solution reservoir; g) H_2 gas bubbler; h) diaphragm injection pump; i) electric heater; j) potentiostat system.
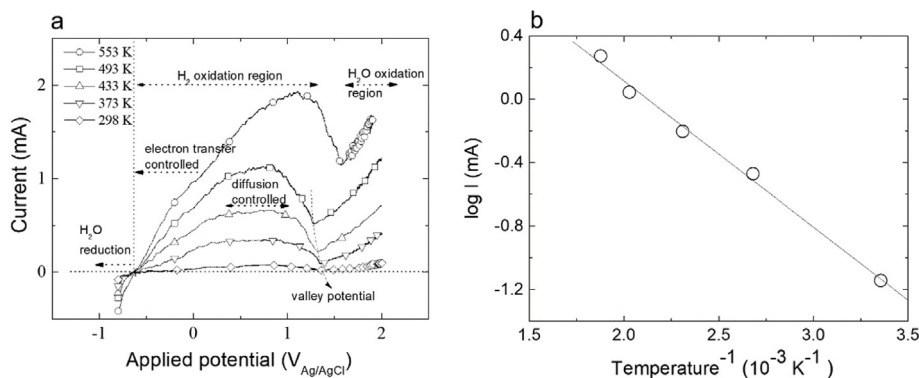
Fig. 2. a Potentiodynamic polarization curves of the Pt electrode in a 32 mM H_3BO_3 solution containing 0.43 mM LiOH hydrogenated with 4.0×10^{-4} M H_2; at 553 K ($\bigcirc$), 493 K ($\square$), 433 K ($\triangle$), 373 K ($\triangledown$) and 298 K ($\diamond$); scan rate, 1 mV s^{-1}; exposed electrode area, 0.1 cm^2 **b** Arrhenius Plot: Reciprocal of temperature and logarithm of diffusion current obtained from Fig. 2a.

electrode in LiOH−H_3BO_3 solutions hydrogenated with 4.0×10^{-4} M H_2 at temperatures of 298 K−553 K. In this figure, the x-axis represents the applied potential value based on the external reference potential. The applied potential was scanned in the anodic direction between −0.8 $V_{Ag/AgCl}$ and 2.0 $V_{Ag/AgCl}$ at a scan rate of 1 mV min^{-1}. Based on the polarization curve at 493 K, the potential region of water reduction was observed below −0.7 $V_{Ag/AgCl}$, the potential region of dissolved H_2 oxidation was observed between −0.6 $V_{Ag/AgCl}$ and +1.2 $V_{Ag/AgCl}$, and the potential region of water oxidation was observed above +1.2 $V_{Ag/AgCl}$. In the polarization curves, reduction and oxidation currents increased overall with an increasing temperature.

In the reduction reaction of water molecules at the Pt electrode, the Volmer step ($H^+ + e \rightarrow H_{ad}$) determines the reaction rate, so the reduction reaction rate is basically affected by the activity of the proton ion (H^+). As the temperature increases, the dissociation of water increases, so the H^+ activity increases. Therefore, it can be understood that as the temperature increases, the water reduction starts at a lower reduction potential and the reduction current increases.

The oxidation potential region of the dissolved H_2 can be further divided into three sub-potential regions. In the first sub-potential region, as the potential increases, the H_2 oxidation current also increases. That is, in the H_2 oxidation reaction (Reaction (1, 2)), Reaction (2) controls the overall reaction rate. In the second region, since the H_2 oxidation current is constant as the applied potential increases, the diffusion of the dissolved H_2 is the rate determining step (RDS). In other words, it is the potential region where Reaction (1) controls the reaction rate in the H_2 oxidation (Reactions (1,2)). In addition, the boundaries of the first and second potential regions for the H_2 oxidation shifted towards the anodic potential with an increasing temperature. This can be interpreted as a phenomenon that occurs because the diffusion current of H_2 increases with the increasing temperature. The third sub-potential region is a peculiar potential region in which the H_2 oxidation current decreases as the applied potential increases. This can be interpreted that the oxidation current of H_2 is reduced by the formation of a Pt oxide (Pt-OH_{ad}, PtO_{ad}, or PtO_2) layer like Reaction (3) in this potential region.

$$H_2 + 2 Pt \rightarrow 2 Pt\text{-}H_{ad} \tag{1}$$

$$Pt\text{-}H_{ad} + H_2O \rightarrow Pt + H_3O^+ + e \tag{2}$$

$$Pt + H_2O \rightarrow Pt\text{-}OH_{ad} + H^+ + e \tag{3}$$

As the solution temperature increases, the oxidation current in the H_2 diffusion-controlled potential region increases. Since this current increase is due to the increase in H_2 diffusion with the increasing temperature, the increase in the diffusion current can be expressed as a function of temperature. In general, mass diffusion such as the diffusion of dissolved gas can be expressed by the Arrhenius equation [16,17], in which the diffusion current is proportional to the reciprocal of the temperature. As shown in Fig. 2b, the diffusion current of H_2 fits the Arrhenius equation. This result confirms once again that the oxidation of H_2 in the plateau potential region is controlled by the diffusion of H_2.

On the other hand, in the oxidation potential region of H_2O, the increase in the oxidation current based on the increase in applied potential greatly increased with the temperature increase. The rate of electron transfer reaction, such as the H_2O oxidation, increased exponentially with the temperature, and the dissociation constant of H_2O also increased with an increasing temperature. Therefore, it can be interpreted that these temperature influence factors contribute to the increase in the oxidation reaction rate of H_2O.

3.2. Effect of dissolved H_2 concentration on the high temperature polarization behavior at the Pt electrode

Fig. 3 shows the potentiodynamic polarization curves of the Pt electrode in the 553 K LiOH−H_3BO_3 solution under various H_2 concentration conditions. The x-axis represents the applied potential value based on the external reference potential. The potential was applied from −0.8 $V_{Ag/AgCl}$ to 2.0 $V_{Ag/AgCl}$ at a scan rate of 1 mV min^{-1} in the positive direction. The polarization curves in Fig. 3 shifted in the direction of the reduction potential as a whole compared to the previous curves (Fig. 2a) because the pH of the solution was adjusted higher than before.

As mentioned in Fig. 2a, the polarization curve of the Pt electrode can be divided into three potential regions, (i.e., water reduction, H_2 oxidation, and water oxidation), as the applied potential increases. In addition, the H_2 oxidation can also be divided into an electron transfer control region, an H_2 diffusion control region, and an H_2 oxidation reduction region by the formation of Pt oxide layer according to the potential increase. These regions slightly shifted toward the oxidation potential as the H_2 concentration increased. The oxidation of the dissolved H_2 started at about −0.6 $V_{Ag/AgCl}$, and the oxidation current of the H_2 increased overall as the H_2 concentration increased.

As shown in Fig. 3, the oxidation reaction rate of the dissolved H_2 is controlled by the electron transfer reaction in the low oxidation potential region and is controlled by the H_2 diffusion in
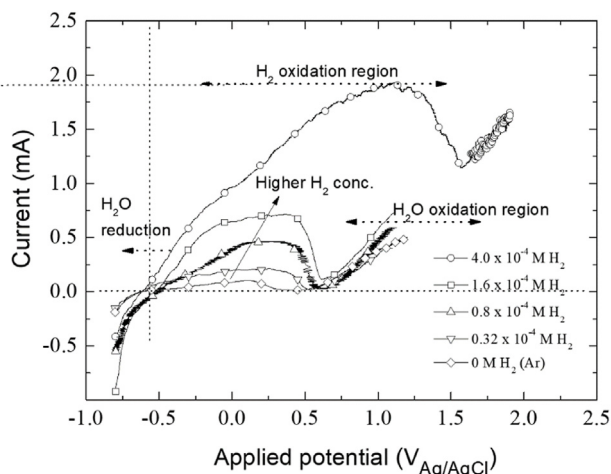
Fig. 3. Potentiodynamic polarization curves of the Pt electrode in a 32 mM H_3BO_3 solution containing 0.43 mM LiOH hydrogenated with hydrogen gas at a solution temperature of 553 K; 4×10^{-4} M H_2 (○), 1.6×10^{-4} M H_2 (□), 0.8×10^{-4} M H_2 (△), 0.32×10^{-4} M H_2 (▽) and 0 M H_2 (◇); scan rate, 1 mV s^{-1}; exposed electrode area, 0.1 cm^2 [15].

the sufficiently high oxidation potential region. In addition, as the concentration of the dissolved H_2 increases, the diffusion current increases, and accordingly, the potential region controlled by the electron transfer reaction becomes wider. As shown in Fig. 4, it can be confirmed again that H_2 oxidation proceeds as a diffusion-controlled reaction from the linear relationship between the dissolved H_2 concentration and the diffusion current (denoted by open square symbol: □).

As the applied potential further increases, the oxidation current of dissolved H_2 decreases, and a valley potential having a minimum current value appears. As the H_2 concentration increases, the minimum current value at the valley potential increases, which indicates that the H_2 oxidation proceeds through the Pt oxide layer even after the formation of the Pt oxide layer is completed. If the thickness and characteristics of the Pt oxide layer are constant regardless of the H_2 concentration, the H_2 concentration and the
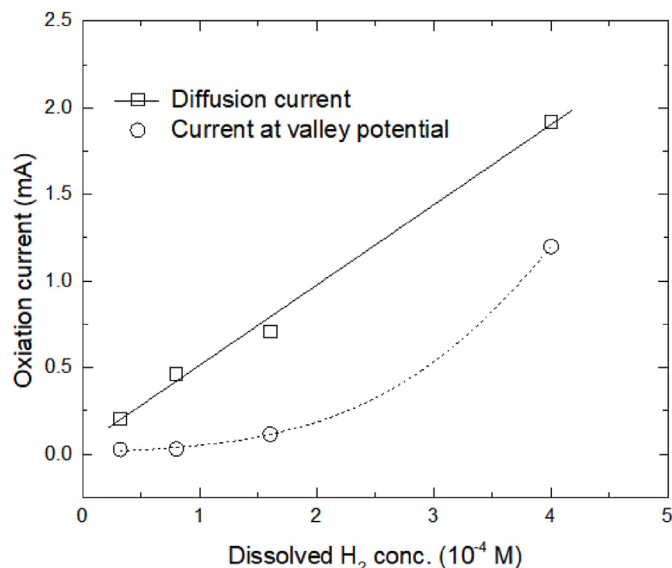
Fig. 4. Oxidation current values according to dissolved H_2 concentration (current data obtained from Fig. 3); diffusion current at plateau (□), current at valley potential (○).

minimum oxidation current value at the valley potential will have a linear relationship. However, the minimum current value (denoted by open circle symbol: ○) shown in Fig. 4 increases exponentially as the H_2 concentration increases. This means that as the H_2 concentration increases, the Pt oxide layer is modified so that H_2 oxidation becomes easier. In other words, this means that when the H_2 concentration increases, the H_2 oxidation causes local environmental changes, such as a decrease of pH on the Pt electrode surface, which consequently affects the properties of the Pt oxide layer.

3.3. Transient current change of H_2 oxidation according to Cl^- concentration

Before the transient experiment, the potentiodynamic polarization curves of the Pt electrode were obtained in 553K hydrogenated LiOH–H_3BO_3 solutions with different Cl^- concentrations. The applied potential was scanned in the direction of the oxidation potential from -0.8 $V_{Ag/AgCl}$ to 1.2 $V_{Ag/AgCl}$ at a scan rate of 1 mV min^{-1}. As shown in Fig. 5a, the polarization curves observed at the Pt electrode that was in the high temperature hydrogenated aqueous solutions were obtained. The influence of the Cl^- concentration was hardly observed on the polarization curves.

The diffusion-controlled current of H_2 oxidation was almost the same regardless of the change in Cl^- concentration. The minimum current value at the valley potential affected by the H_2 concentration showed a slight difference at a high Cl^- concentration, but a current difference at a low Cl^- concentration was difficult to distinguish. In conclusion, it was difficult to confirm the effect of Cl^- ions concentration on the H_2 oxidation reaction with a steady-state measurement technique such as potentiodynamic polarization.

Fig. 6 shows the current-time transient curve measured after applying the oxidation potential to the Pt electrode in the same solution as in the experiment in Fig. 5a. Here, the transient current is the current measured after momentarily shifting the potential of the Pt electrode from the potential without an oxide layer (-0.65 $V_{Ag/AgCl}$) to the valley potential where a Pt oxide layer is formed ($+0.55$ $V_{Ag/AgCl}$). For all Cl^- containing solutions, the transient current of the dissolved H_2 oxidation showed an exponential decreasing shape with time. In addition, as the Cl^- ion concentration increased, the initial maximum current and the accumulated oxidation charge up to 1.0 s increased, respectively.

When a valley potential was applied to the Pt electrode, the oxidation of the dissolved H_2 and the oxidation of the Pt surface took place simultaneously. Therefore, this rapid decrease in transient current can be understood as a result of the H_2 oxidation slowing down significantly as the formation of the Pt oxide layer was completed. It is known that the surface oxidation process of Pt is that a thin Pt oxide layer such as Pt-OH_{ad} is formed first, and then a thick PtO_2 oxide layer is formed as a bilayer on top of the thin oxide layer [18]. In addition, during the formation of the Pt oxide layer, the Cl^- ions hinder the bonding of Pt and OH^- (or H_2O), so the growth of both thin and thick Pt oxide layers will be delayed. From the relationship among the Cl^- ion, Pt oxide layer, and H_2 oxidation, it is possible to clearly understand the phenomenon that the transient current changes significantly according to the Cl^- ion concentration.

During the growth of the Pt oxide layer, a difference in oxidation current was observed depending on the Cl^- concentration as shown in Fig. 6, whereas after the oxide layer growth was completed (at 0.5 s) on the Pt surface where the current was constant, the oxidation current was the same regardless of the Cl^- concentration. This means that Cl^- ions affect the growth rate of the Pt oxide layer, but unlike H_2, they do not significantly affect the thickness or characteristics of the Pt oxide layer.

In Table 1, the initial maximum oxidation current after applying
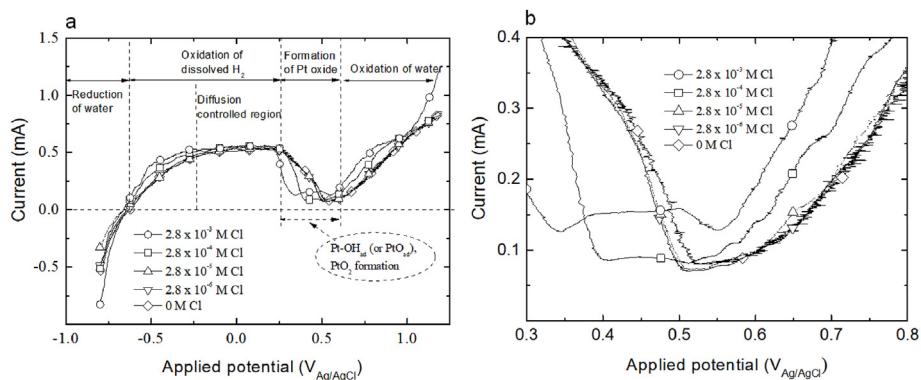
Fig. 5. a Potentiodynamic polarization curves of the Pt electrode in a 32 mM H_3BO_3 solution containing 0.43 mM LiOH hydrogenated with 1.6×10^{-4} M H_2 and with chloride ion at a solution temperature of 553 K: 2.8×10^{-3} M ($\bigcirc$), 2.8×10^{-4} M ($\square$), 2.8×10^{-5} M ($\triangle$), 2.8×10^{-6} M (∇) and 0 M Cl^- ion ($\diamond$); scan rate, 1 mV s^{-1}; exposed electrode area, 0.1 cm^2 **b** An enlarged view of the current in the valley potential region of Fig. 5a.
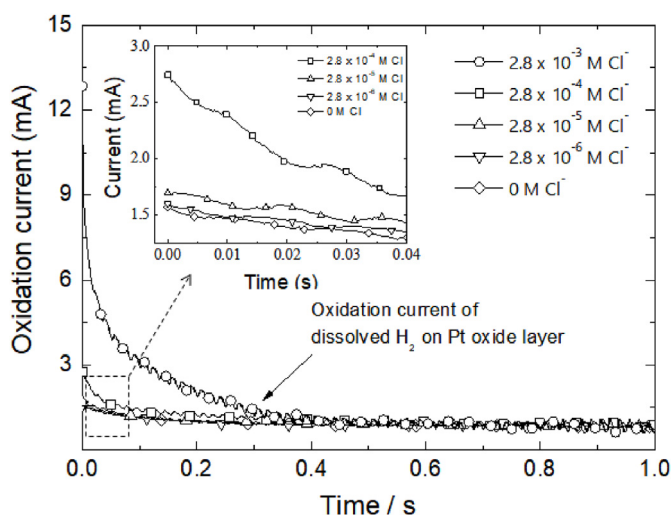
Fig. 6. Chronoamperometric curves obtained at Pt in a 32 mM H_3BO_3 solution containing 0.43 mM LiOH hydrogenated with 1.6×10^{-4} M H_2 at 553 K, the potential shift from -0.65 $V_{Ag/AgCl}$ to $+0.55$ $V_{Ag/AgCl}$. Chloride ion concentrations of 2.8×10^{-3} M ($\bigcirc$), 2.8×10^{-4} M ($\square$), 2.8×10^{-5} M ($\triangle$), 2.8×10^{-6} M (∇) and 0 M Cl^- ion ($\diamond$), exposed electrode area of 0.1 cm^2.
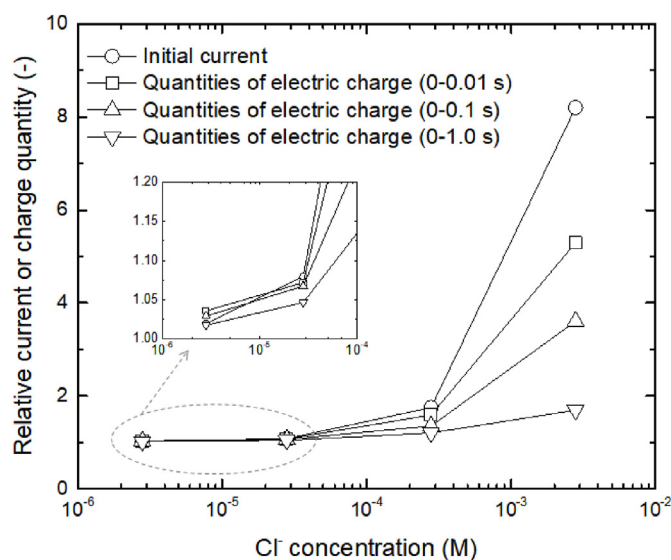
Fig. 7. Relative current or QEC (quantities of electric charge) according to Cl^- concentration, calculated from data in Table 1. Initial current value ($\bigcirc$), QEC of 0−0.01 s ($\square$), 0−0.1 s ($\triangle$), and 0−1.0 s (∇).

the valley potential and the quantities of electric charges after 0.01 s, 0.1 s, and 1.0 s were compared according to the Cl^- concentration. In Fig. 7, the calculated values obtained according to the Cl^- concentration are compared based on the value when the Cl^- concentration is 0, and the log-log relationship is shown. The shorter the cumulative time, (in the order of initial maximum

oxidation current, quantities of electric charges for 0.01 s, 0.1 s, and 1.0 s), the more sensitive the transient current (or charge) responded to the Cl^- concentration. This indicates that Cl^- ions are more affected in the initial stage of oxide layer growth, which is the formation of a thin Pt oxide layer, than in the stage of forming a thick oxide layer.

From our experimental results, it is difficult to quantitatively identify the effect of Cl^- concentration on the growth rate of the Pt oxide layer and the relationship between the growth of the Pt oxide layer and H_2 oxidation current. However, our current transient results clearly show that the Cl^- concentrations in high temperature hydrogenated solutions can be detected up to at least 2.8×10^{-5} M.

4. Conclusions

The potentiodynamic polarization curve of the Pt electrode in a hydrogenated high temperature LiOH−H_3BO_3 solution was largely divided into three potential regions: Water reduction, dissolved H_2 oxidation, and water oxidation. The current in these three potential

Table 1
Initial current (t = 0 s) and quantities of electric charges according to Cl^- ion concentration.

Cl^- conc. (µM)	Current (mA) at t = 0	Quantity of electric charge (mC)		
		0−0.01 s	0−0.1 s	0−1.0 s
0	1.57	0.0167	0.1303	0.9166
2.8	1.60	0.0173	0.1341	0.9328
28	1.69	0.0179	0.1391	0.9594
280	2.740	0.0266	0.1765	1.1055
2800	12.844	0.0884	0.4699	1.5538

regions increased with an increasing temperature up to 553 K. There was a diffusion-controlled region in the oxidation potential region of the dissolved H_2. In addition, the logarithmic value of the diffusion current of the dissolved H_2 showed a linear relationship with the reciprocal of the temperature. It was confirmed that there was a potential region in which the H_2 oxidation current decreased even when the applied potential increased due to the Pt oxide layer that formed in the valley potential between the H_2 oxidation and the water oxidation region.

The H_2 oxidation current at the Pt electrode increased as the concentration of dissolved H_2 increased in the high temperature $LiOH−H_3BO_3$ solution. The diffusion current of the H_2 showed a linear relationship with the concentration of the dissolved H_2, but the current value at the valley potential did not show a linear relationship with the H_2 concentration. This means that the thickness or characteristics of the Pt oxide layer that formed in the valley potential differs depending on the concentration of the dissolved H_2.

It was difficult to detect $Cl^−$ concentrations below 2.8×10^{-3} M with the polarization curves measured at a steady-state condition in hydrogenated high temperature solutions. However, the transient currents of H_2 oxidation measured during the growth of the Pt oxide layer were able to detect $Cl^−$ concentrations as low as 2.8×10^{-5} M. This is because even a very low concentration of $Cl^−$ ions can affect the growth rate of the Pt oxide layer.

Declaration of competing interest

The authors declare that they have no known competing financial interests or personal relationships that could have appeared to influence the work reported in this paper.

Acknowledgments

References

[1] C.J. Wood, PWR Primary Water Chemistry Guidelines: Revision 3, Electric Power Research Institute, Palo Alto, CA, USA, 1995. Report EPRI TR-105714.

[2] K. Ishigure, T. Nukii, S. Ono, Analysis of water radiolysis in relation to stress corrosion cracking of stainless steel at high temperatures − effect of water radiolysis on limiting current densities of anodic and cathodic reactions under irradiation, J. Nucl. Mater. 350 (2006) 56−65.

[3] G.D. Fearnehough, A. Cowan, The effect of hydrogen and strain rate on the "ductile-brittle" behaviour of Zircaloy, J. Nucl. Mater. 22 (1967) 137−147.

[4] A. Cowan, W.J. Langford, Effect of hydrogen and neutron irradiation on the failure of flawed Zircaloy-2 pressure tubes, J. Nucl. Mater. 30 (1969) 271−281.

[5] E. Smith, Near threshold delayed hydride crack growth in zirconium alloys, J. Mater. Sci. 30 (1995) 5910−5914.

[6] T. Magnin, D. Noël, R. Rios, Microfractographic aspects of stress corrosion cracking of Inconel 600 in a pressurized water reactor environment, Mat. Sci. Eng. A-Struct. 177 (1994) L11−L14.

[7] D.M. Symons, The effect of hydrogen on the fracture toughness of alloy X-750 at elevated temperatures, J. Nucl. Mater. 265 (1999) 225−231.

[8] K.A. Burrill, Some aspects of water chemistry in the CANDU primary coolant circuit, in: Proceedings of JAIF International Conference on Water Chemistry in Nuclear Power Plants, Kashiwazaki, Japan, 1998. October 13-16.

[9] J.-W. Yeon, Y. Jung, S.-I. Pyun, Deposition behaviour of corrosion products on the Zircaloy heat transfer surface, J. Nucl. Mater. 354 (2006) 163−170.

[10] D.M. Symons, The effect of hydrogen on the fracture toughness of alloy X-750 at elevated temperatures, J. Nucl. Mater. 265 (1999) 225−231.

[11] J.O.'M. Bockris, A.K. Reddy, Modern Electrochemistry, Plenum/Resetta ed., Plenum Press, New York, 1973.

[12] E. Gileadi, E. Kirowa-Eisner, J. Penciner, Interfacial Electrochemistry, Addison-Wesley Publishing Company, London, 1975.

[13] B.E. Conway, L. Bai, Determination of adsorption of OPD H species in the cathodic hydrogen evolution reaction at Pt in relation to electrocatalysis, J. Electroanal. Chem. 198 (1986) 149−175.

[14] J.-W. Yeon, S.-I. Pyun, Roles of adsorbed OH and adsorbed H in the oxidation of hydrogen and the reduction of UO2+2ions at Pt electrodes under non-conventional conditions, J. Appl. Electrochem. 37 (2007) 905−912.

[15] J.-W. Yeon, M.H. Yun, K. Song, Introduction to a new real-time water chemistry measurement system, in: 15th International Conference on Environmental Degradation of Materials in Nuclear Power Systems - Water Reactors, Colorado Springs, USA, 2011. August 7-11.

[16] W.M. Flarsheim, Y. Tsou, I. Tratchtenberg, K.P. Johnston, A.J. Bard, Electrochemistry in near-critical and supercritical fluids. 3. Studies of bromide, iodide, and hydroquinone in aqueous solutions, J. Phys. Chem. 90 (1986) 3857−3862.

[17] C. Liu, S.R. Snyder, A.J. Bard, Electrochemistry in near-critical and supercritical fluids. 9. Improved apparatus for water systems (23−385 °C). The oxidation of hydroquinone and iodide, J. Phys. Chem. B 101 (1997) 1180−1185.

[18] H.A. Baroody, G. Jerkiewicz, M.H. Eikerling, Modelling oxide formation and growth on platinum, J. Chem. Phys. 146 (2017), 144102.